Tensile behaviour of polyethylene and poly(p-xylylene) fibres

van der Werff, Harm

Chapter 6

CREEP RESISTANCE AND HIGH TEMPERATURE STRENGTH OF HIGH STRENGTH AND HIGH MODULUS POLY(P-XYLYLENE) FIBRES

6.1 Summary

High strength and high modulus poly(p-xylylene) (PPX) fibres show no creep at room temperature and retain at 200 ^{0}C, in air or in nitrogen atmosphere, still 50 to 60 % of their tensile strengths at room temperature, whereas the modulus does not change. In stress relaxation experiments PPX fibres have relaxed after 17.4 hours less than 4 % of the initial stress whereas during the same period of time polyethylene fibres relax over 75 % of the initial stress.

6.2 Introduction

High strength and high modulus PPX fibres can be readily prepared by hot-drawing of the high molecular weight as-polymerized material [1]. Tensile strengths of 3.0 GPa and moduli of 100 GPa can be achieved. Up to now, interest in PPX has been mainly aroused by its unique polymerization process [2,3] and its high resistance towards electron beam irradiation [4]. This last property permitted the material to be studied by high resolution electron microscopy, in single crystals [5-7] or in hot-drawn fibres [8].

The aim of the work presented in this paper is to explore properties of PPX fibres with respect to creep and high temperature strength. These properties can be of crucial importance for technological applications of polymeric fibres. High strength and high modulus fibres of ultra-high molecular weight polyethylene (UHMWPE) can be prepared by gel-spinning and consequent hot-drawing [9]. Although a tensile strength of 7.2 GPa [10] and a Young's modulus of 264 GPa [11] can be achieved at room temperature, these fibres have some disadvantages: tensile strength decreases significantly with increasing temperature and is zero at temperatures above 152 ^{0}C [12]. Furthermore, UHMWPE fibres are very susceptible to creep [13]. Poly(p-phenylene terephtalamide) fibres show essentially no creep

and excellent high temperature strength, but have to be spun from solutions in concentrated sulphuric acid [14]. It is therefore of technological interest to examine additional fibre properties, apart from tensile strength and modulus, and compare these to properties of other fibres in order to estimate the full potential of PPX as a strong polymeric material.

6.3 Experimental

High strength PPX fibres were prepared by drawing of the as-polymerized material at 420 ^{0}C, as described previously [1]. As-polymerized PPX was kindly supplied to us by Union Carbide Co.. Gel-spun UHMWPE fibres were prepared by standard procedures in our laboratory [9] from linear polyethylene Hifax 1900 (M_w= 5.5x10^6 kg/kmol, $M_w/M_n \approx$ 3). Cross-sectional areas of filaments were determined from fibre weight and length. Tensile tests and stress relaxation experiments were performed using an Instron 4301 tensile tester, equipped with a temperature cabinet, at a gauge length of 32.5 mm. For the dead load experiments, a piece of fibre was clamped at both ends. One of the clamps was fixed in position, whereas the other was freely suspended and had various weights attached. The movement of the latter was recorded by means of a linear displacement transducer coupled to a x-t recorder. Scanning electron microscopy (SEM) micrographs were taken using an ISI-DS 130 microscope operating at 40 kV, from gold-covered samples.

6.4 Results and discussion

As-polymerized PPX at room temperature exhibits plastic deformation upon tensile testing. The stress-strain curve in figure 6.1 indicates ductile behavior and can be divided into three stages: elastic deformation ($<$ 1.5 % strain), followed by plastic deformation (1.5-4.0 % strain) and finally crack formation leading to tensile failure ($>$ 4.0 %). The successive transitions between these stages have been indicated by A and B in figure 6.1. SEM micrographs clearly identify the three stages. Figure 6.2 shows the existence of localized surface plastic zones, initiated at surface defects, and cracks formed inside these plastic deformation zones. Figure 6.3 clearly reveals the existence of fibrils inside the plastic deformation

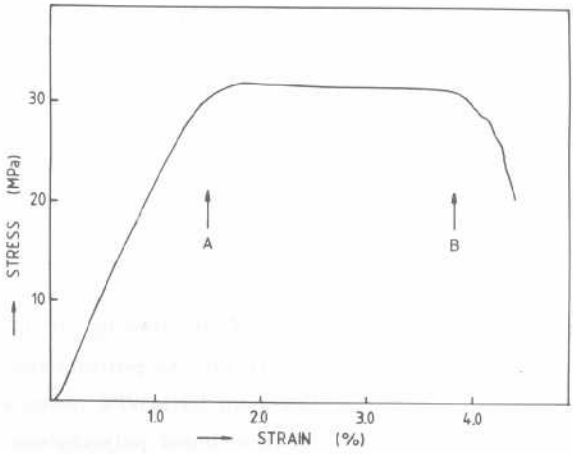

Figure 6.1 *Stress versus strain of as-polymerized PPX. Cross-head speed : 3.25 mm/min.*

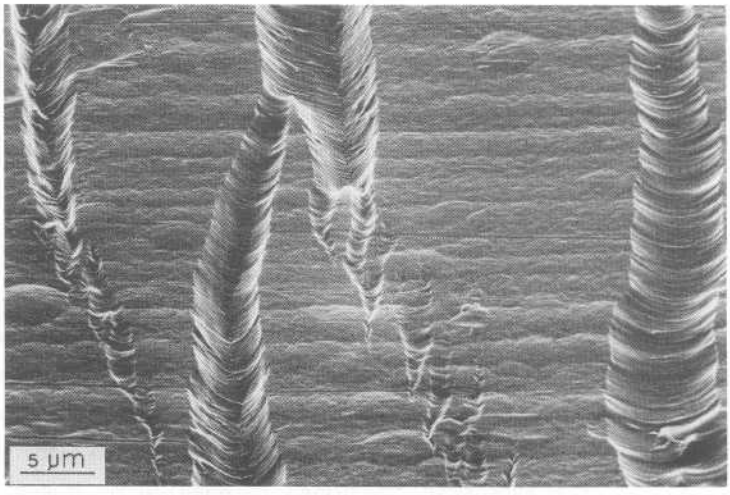

Figure 6.2 *SEM-micrograph of as-polymerized PPX after tensile deformation showing plastic zones in different stages of development. Draw direction is horizontal.*

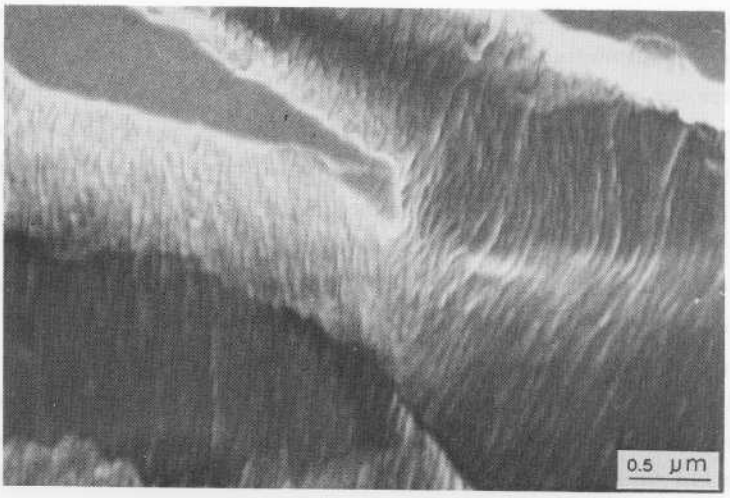

Figure 6.3 *SEM-micrograph of as-polymerized PPX after tensile deformation. Fibrils of about 50 nm in diameter appear to be directly formed without noticeable voiding.*

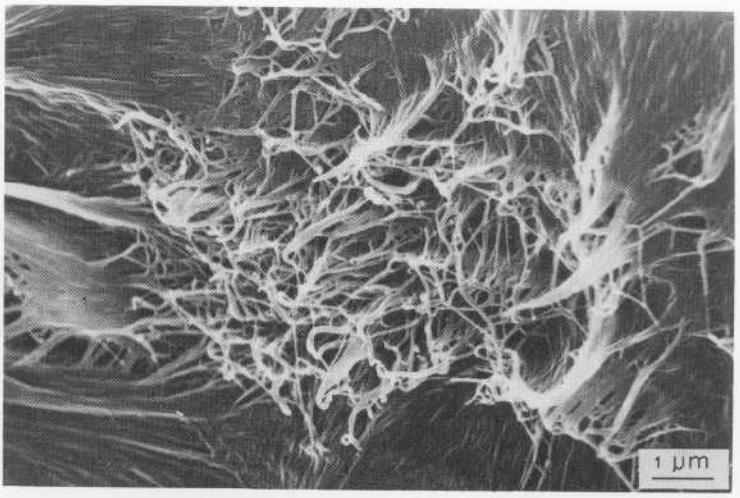

Figure 6.4 *SEM-micrograph of fracture surface of as-polymerized PPX after tensile deformation, showing the formation of fibrils and voids by crack growth.*

zones prior to crack growth, and appear to be formed without noticeable formation of voids. Probably, fibrils are easily formed due to the low entanglement density in the as-polymerized material. The fracture surface is shown in figure 6.4 and displays the extensive fibrillation and creation of voids due to crack growth [15]. The results from figure 6.1 to 6.4 indicate that, at room temperature, unoriented PPX responds by flow of the polymeric chains upon tensile deformation.

Tensile deformation at temperature close to the melting point (T_m= 427 °C [16]) of PPX results into extensive flow and the material can be drawn up to draw-ratio λ of 43 [1]. Hot-drawn PPX fibres then have a high tensile strength σ_b and modulus, and break brittle at room temperature. Figure 6.5 is a plot of strain versus time during a dead-load test of a PPX fibre (λ=30, σ_b= 2.3 GPa) and a UHMWPE fibre (λ=30, 1.5 wt. % gel, σ_b= 2.3 GPa). The load applied corresponds in both cases to 60 % of the load at break. The plot shows the extensive creep strain (up to 20 %) and the short time to break (1 hour) of the UHMWPE fibre. The PPX fibre, having comparable tensile properties, responds dramatically different to the application of the load. An elastic strain of about 1.6 % results, but there is no tendency to increase its length in time. Even after 306 hours, no creep strain could be measured within the accuracy of the experimental set-up (0.1 %

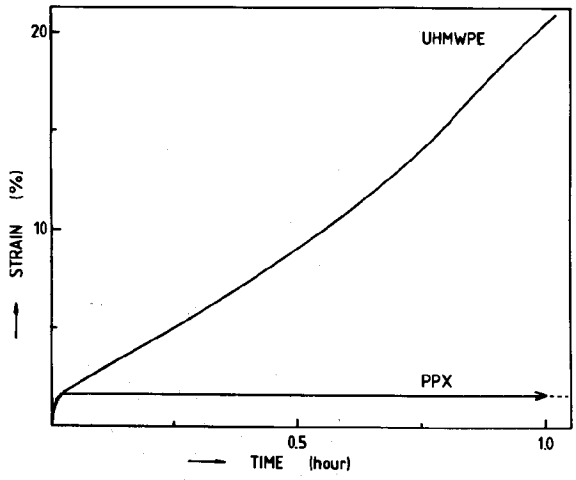

Figure 6.5 *Strain versus time of PPX and UHMWPE fibres during a dead-load test. Both fibres, having a tensile strength of 2.3 GPa, had loads attached corresponding to 60 % of the load at break.*

strain) and the experiment was stopped before fibre failure occurred.

The high resistance to flow of chains in oriented PPX fibres is also demonstrated by stress relaxation. In figure 6.6, the stress, as a percentage of the stress at which the crosshead was stopped, is plotted as a function of time, after the fibres had been elongated to result in a tensile stress corresponding to 60 % of the tensile strength. The UHMWPE fibre (λ=30, 1.5 wt. % gel, σ_b= 2.3 GPa) again displays the ease of flow in these fibres, for it can relax over 75 % of its intitial stress during 17.4 hours, whereas the PPX fibre (λ=29, σ_b= 2.1 GPa) is only able to relax about 3.6 % of its initial stress during the same period of time.

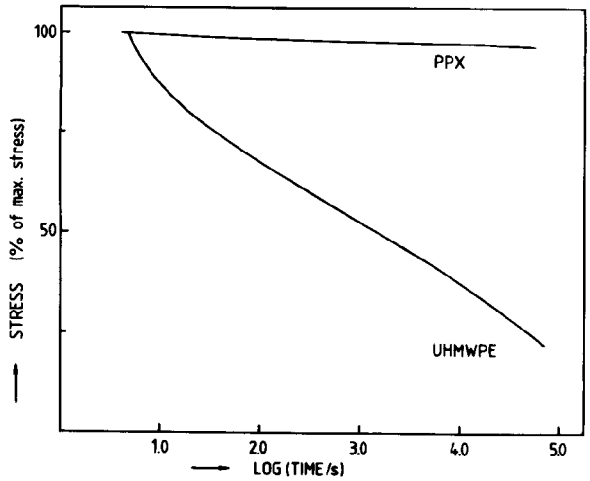

Figure 6.6 *Stress versus log(time) during stress relaxation of PPX and UHMWPE fibres. Both fibres were stressed up to 60 % of their tensile strengths (2.1 and 2.3 GPa respectively). Cross-head speed : 10 mm/min. Zero time corresponds to the start of the crosshead movement.*

UHMWPE fibres have zero tensile strength above 152 ^{0}C, the temperature at which the orthorhombic crystals transform into the hexagonal phase [12]. In this phase, chains can slip past each other, and the fibres will directly melt. Table 6.1 lists some tensile strengths and moduli of PPX fibres tested at a temperature of 200 ^{0}C. Fibres have been tested as well in nitrogen atmosphere as in air. Tensile testing normally took place several minutes after the introduction of the fibres into the preheated temperature cabinet. The data in table 6.1 indicate that under these conditions PPX fibres still retain about 50-60 % of their original tensile

Table 6.1

Tensile strength σ_b and Young's modulus E of PPX fibres at different temperatures. The values at T = 20 °C were derived from figures 4.7 and 4.8.

Draw ratio	T = 20 °C	T = 200 °C	Atmosphere
31	σ_b = 2.3 GPa E = 90 GPa	σ_b = 1.4 GPa E = 90 GPa	nitrogen
35	σ_b = 2.5 GPa E = 93 GPa	σ_b = 1.2 GPa E = 99 GPa	air

strengths at room temperature. The modulus is not affected by the elevated temperature. A stress-strain curve recorded at 200 °C in nitrogen atmosphere is shown in figure 6.7. The stress-strain curve still shows no yielding behaviour. The strain at break of 1.6 % is much smaller than the strain at break of about 3 % normally found at room temperature. Probably flaws in the fibres become increasingly fatal at higher temperatures, causing fracture at lower strains.

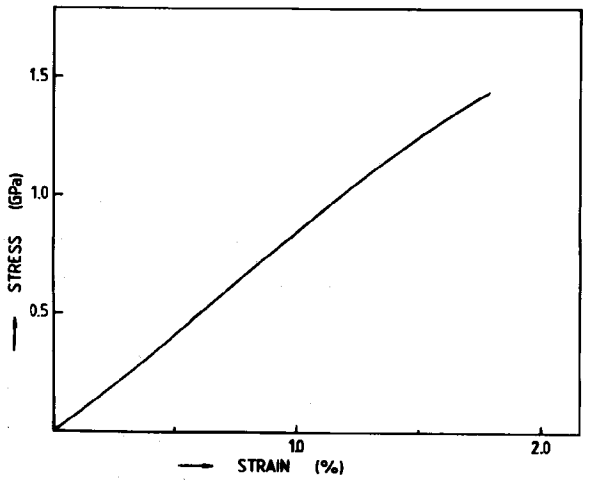

Figure 6.7 *Stress versus strain of a PPX fibre at 200 °C in nitrogen atmosphere. The corresponding strength at room temperature is 2.3 GPa. Cross-head speed : 10 mm/min.*

Tensile testing of PPX fibres from the same batch at room temperature however also gave rise to the same behaviour as shown in figure 6.7. The low stress and strain at break then must have been caused by aging or degradation phenomena during storage. The samples had been stored in closed glass tubes in the dark during 3 years. This may even indicate that the tensile strength of PPX fibres is the same at 200 ^{o}C as at room temperature. Because further samples were not available, these findings could not be examined more explicitly.

6.5 Conclusions

The results presented here show that the as-polymerized material responds at room temperature in a ductile manner to tensile deformation. Oriented PPX fibres, however, are much less susceptible to flow, and are by far superior to UHMWPE fibres with respect to creep, stress relaxation and high temperature strength. The high melting point of 427 ^{o}C of PPX [16] indicates the difficulty of a chain at room temperature to slip out of its crystal lattice, despite the absence of dipolar interactions and hydrogen bonding between neighbouring chains.

Combined with the fact that PPX fibres can be easily prepared in one step from as-polymerized films and no additional dissolution in a solvent is required to obtain a drawable precursor material, these results demonstrate the vast potential of PPX as a strong polymeric material.

5.6 References

1. H. van der Werff, A.J. Pennings, Polym. Bull., 19, 587 (1988).
2. M. Szwarc, Discussions Faraday Soc., 2, 48 (1947).
3. W.F. Gorham, J. Polym. Sci. Part A-1, 3027 (1966).
4. M. Tsuji, S. Isoda, M. Ohara, A. Kawaguchi, K. Katayama, Polymer, 23, 1568 (1982).
5. G.A. Bassett, A.A. Keller, Kolloid Z., 231, 386 (1969).
6. S. Isoda, T. Ichida, A. Kawaguchi, K. Katayama, Bull. Inst. Chem. Res. Kyoto Univ., 61, 222 (1983).
7. S. Isoda, M. Tsuji, M. Ohara, A. Kawaguchi, K. Katayama, Polymer, 24, 1155;

idem, Makromol. Chem. Rapid Comm., 4, 141 (1983).

8. H. van der Werff, A.J. Pennings, G.T. Oostergetel, E.F.J. van Bruggen, J. Mat. Sci. Lett., 8, 231 (1989).
9. J. Smook, M. Flintermann, A.J. Pennings, Polym. Bull., 2, 775 (1980).
10. A.J. Pennings, M. Roukema, A. van der Veen, Polym. Bull., 23, 353 (1990).
11. H. van der Werff, A.J. Pennings, Colloid Polym. Sci., submitted.
12. D.J. Dijkstra, J.C.M. Torfs, A.J. Pennings, Colloid Polym. Sci., 286, 866 (1989).
13. I.M. Ward, M.A. Wilding, J. Polym. Sci. Polym. Phys. Ed., 22, 561 (1984).
14. M.G. Northolt, D.J. Sikkema, "Lyotropic Main Chain Liquid Crystal Polymers", in: A.A. Collyer (ed.) Liquid Crystal Polymers, Elseviers Applied Science, to be published.
15. E.J. Kramer, "Microscopic and Molecular Fundamentals of Crazing", in: H.H. Kausch (ed.) Crazing in Polymers, Springer, Berlin Heidelberg New York, Advances in Polymer Science, 52/53, pp. 1-56 (1983).
16. D.E. Kirkpatrick, B. Wunderlich, Makromol. Chem., 186, 2595 (1985).